ACS Sustainable Chemistry & Engineering

Research Article

pubs.acs.org/journal/ascecg

Removal of Arsenic and Phosphate from Aqueous Solution by Metal (Hydr-)oxide Coated Sand

Yuxiong Huang,[†] Jae-Kyu Yang,[‡] and Arturo A. Keller*[,†]

[†]Bren School of Environmental Science and Management, University of California at Santa Barbara, California 93106, United States

[‡]Division of General Education, Kwangwoon University, Seoul 139-701, Korea

Supporting Information

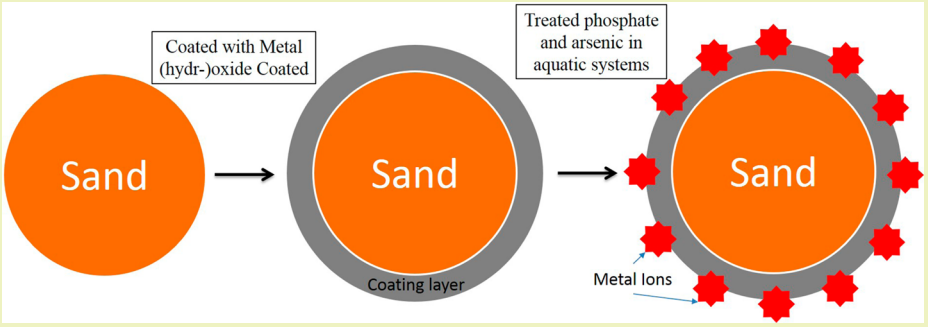

ABSTRACT: Arsenic contamination is a major concern in many drinking water supplies around the world. One low-cost approach for removing arsenic and other oxyanions such as phosphate is to use metal (hydro-)oxide coated sands. In this study, solution pH, sand grain size, coating efficiency, and mineral type for iron-coated sand (ICS), manganese-coated sand (MCS), and iron- and manganese-coated sand (IMCS) were evaluated. Scanning electron microscopy (SEM) and X-ray diffraction (XRD) analysis were used to investigate the surface properties of the coated layer. The mineral type of ICS prepared at different solution pH was identified as a mixture of FeOOH and Fe_2O_3. The mineral type of MCS prepared at pH 4 and 7 was identified as MnO_2 and changed to ramsdellite (γ-MnO_2, a mixture of α-MnO_2 and β-MnO_2) at pH 10. ICS exhibited a greater phosphate removal capacity, and phosphate removal increased with increasing iron oxide on the sand. ICS was also shown to have a greater removal capacity for phosphate than chemical precipitation methods by $FeCl_3$, especially below neutral pH. In contrast, IMCS(Fe:Mn = 7:3) was better for removing As(III), which occurs through oxidation to As(V) and adsorption of As(III) and As(V) and can reach >98% removal rate (residual concentration <0.02 mg/L) at neutral pH. IMCS(7:3) is an efficient adsorbent for arsenic, as >50% can be removed within 60 min; 66% adsorption was reached after 24 h. Removal of arsenic and phosphate by these metal (hydro-)oxide coated sand adsorbents followed a pseudo-second-order rate and Langmuir as well as Freundlich adsorption isotherms. Removal under different conditions (e.g., pH, ionic strength) was also evaluated to provide information to optimize the process.

KEYWORDS: *Adsorption, Iron-coated sand, Manganese-coated sand, Arsenic, Phosphate, Water treatment*

INTRODUCTION

Arsenic is a contaminant in soil and water systems due to natural geochemical and anthropogenic sources, such as mining activity, discharges of industrial wastes, and agricultural application of fertilizers.[1] Elevated concentrations of arsenic have also been found in water systems originating from natural sources.[2] Arsenic contamination in groundwater is a worldwide concern because the metal may have severe adverse effects on human and ecological receptors.[3] Primary potable water supplies are contaminated in many rural areas and developing countries like Bangladesh, India, and Nepal, where the arsenic level has remained at 50 μg/L.[4,5] Bangladesh is in a severe situation, with 35−77 million of its citizens potentially exposed to water with arsenic levels above the recommended limit of the World Health Organization (WHO), which is 10 μg/L.[6,7] Facing the technical and economic challenges associated with achieving this standard, the development of novel technologies to remove arsenic contaminants from water in a sustainable and economical way is of great importance.

Although arsenic has multiple oxidation states (+5, +3, +2, 0, and −3),[8] arsenite As(III) and arsenate As(V) are the most common states in natural environments.[9] Generally, As(III) is the common species under anaerobic conditions, while the As(V) species occurs under aerobic conditions.[10] Speciation and solubility of inorganic arsenic is sensitive to both redox conditions and pH of the environment, which affects the toxicity and mobility of arsenic in soils.[10,11] In order to treat arsenic in water systems, several natural and synthetic iron- and

Received: November 19, 2013
Revised: February 23, 2014
Published: April 8, 2014

manganese-containing adsorbents have been considered recently.[12,13] Sand media coated with hematite and goethite (ICS, iron-coated sand) showed significant removal capacities for As(III) and As(V) through adsorption. MCS (manganese-coated sand) coated with pyrrolusite (δ-MnO_2) showed good As(III) oxidation efficiency but much less adsorption capacity for As(V).[14] Therefore, it may be more efficient to combine ICS and MCS to enhance both oxidation and adsorption processes at the same time.

Contamination of surface water bodies by excess phosphorus, an essential macronutrient, from domestic wastewater discharges, agricultural drainage, and urban runoff, can cause widespread eutrophication of lakes and seas.[15] Eutrophication due to municipal and industrial wastewater was reported[16] even at low concentrations of phosphate (less than 1 mg/L as phosphorus). For the removal of phosphorus from water and wastewater, several methods such as conventional activated-sludge, precipitation with lime and salts of aluminum or iron, and ion exchange processes have been employed.[17−20] However, these conventional methods cannot meet current more-stringent phosphate control regulations (i.e., U.S. EPA Actions Regarding Numeric Nutrient Criteria for Florida), which require levels as low as 0.1 mg/L as total phosphorus (TP).[21] Therefore, more effective treatment of wastewater containing residual inorganic phosphates is needed.

The objective of this study was to investigate the effect of different sand coating ratios of iron and manganese on the removal of arsenic and phosphate from aqueous solution in a batch reactor, considering ICS alone, MCS alone and IMCS (iron and manganese coated sand). Optimizing the synthesis protocol, we lowered the metal (hydr-)oxide coated sand preparation temperature to make production more sustainable (i.e., less energy) and economical. By evaluating the adsorption performance at different ratios of coated iron and manganese, we enhanced both adsorption and oxidation behavior in the treatment system. The properties of different sand media were analyzed using a scanning electron microscopy (SEM), surface area analyzer and an X-ray diffractometer (XRD). Equilibrium, kinetic and effect of pH batch experiments were performed to examine the adsorption of arsenic and phosphate to ICS, IMCS and MCS.

MATERIALS AND METHODS

Materials. QUIKRETE All-Purpose Sand (No. 1152) was used as the supporting material for iron and manganese. This sand was sieved into three different ranges of particle sizes: fine (100−125 μm), medium (425−500 μm), and coarse (850−1000 μm). Prior to coating the iron and manganese onto the sand, the raw sands were soaked in 0.1 M HCl for 2 h and rinsed two times with deionized water to remove impurities. All chemicals were analytical grade. Na_3PO_4, $FeCl_3$, $Mn(NO_3)_2$, As_2O_3, and $NaAsO_2$ were purchased from Alfa Aesar (U.S.A.). NaH_2PO_4 was obtained from Bigelow Laboratory for Ocean Sciences (U.S.A.). $NaNO_3$, used to adjust ionic strength, was obtained from EMD Millipore (U.S.A.). NaCl and Na_2SO_4 were purchased from Fisher Scientific (U.S.A.). Dowex 1 × 8 50−100 mesh ion-exchange resin was purchased from Acros Organics (U.S.A.). All solutions were prepared with deionized water (18 MΩ cm) prepared using a Barnstead NANOpure Diamond Water Purification System (U.S.A.).

Preparation of ICS, MCS, and IMCS. For preparing ICS, a $FeCl_3$ solution (100 mL, 0.1 M), adjusted to pH 4, 7, or 10 with 0.1 M HNO_3 or NaOH, was mixed with raw sand (100 g) in a rotary evaporator for 2 h. For MCS, a $Mn(NO_3)_2$ solution (100 mL, 0.1 M), previously adjusted to pH 4, 7 or 10, was mixed with raw sand (100 g) in the rotary evaporator. For IMCS, $FeCl_3$ (50 mL, 0.1 M) and $Mn(NO_3)_2$ (50 mL, 0.1 M) solutions, previously adjusted to pH 4, were mixed at different ratios with raw sand (100 g) in the rotary evaporator. While rotating each suspension at 30 rpm (revolutions/min) in a water bath maintained at 80 °C, water was continuously removed by applying a vacuum until approximately 10−15% of water remained in the suspension. Thereafter, the sand was dried at 150 °C for 3 h. (This second coating step temperature was much lower than previous research, which was 550 °C[22]). In order to remove traces of uncoated iron or manganese, the dried coated sand was rinsed three times with distilled water and then dried again at 105 °C.

To determine the amount of iron and manganese deposited on the coating, an acid digestion method (U.S.EPA 3050B) was used to strip manganese and iron coated from each sand. After filtration (with 1.2 μm Whatman glass microfiber filters), the dissolved concentrations of manganese and iron were measured using inductively coupled plasma with atomic emission spectroscopy (ICP-AES, Thermo iCAP 6300).

The mineral types of ICS, MCS, and IMCS were characterized by X-ray diffraction (XRD, Bruker D8 Advance). Photomicrography and inorganic characterization of the raw sand, ICS, MCS, and IMCS were obtained by scanning electron microscopy (SEM, FEI XL40 Sirion FEG digital scanning microscope with EDS). Brunauer−Emmett−Teller (BET) surface areas, porosities, and pore sizes were determined using a computer-controlled nitrogen gas adsorption analyzer (TriStar 3000). pH_{pzc} (pH at point of zero charge) values of the adsorbents were measured using a Malvern Zetasizer Nano ZS90.

Batch Adsorption Studies. Adsorption of arsenic or phosphate onto ICS, IMCS, and MCS was performed at various solution pH. Each adsorbent (0.25 g) was mixed with 50 mL of arsenic (1 mg/L As(III)) or phosphate (2 mg/L) solution, and the solution pH was varied from 3 to 10 using 0.01 M HCl or NaOH to adjust pH. Then, the solutions were placed in a rotator maintained at constant 30 rpm for 24 h. From the kinetics experiments, 24 h was determined as a sufficient equilibration time. All experiments were conducted at a fixed ionic strength (0.01 M $NaNO_3$ for phosphate and 0.01 M NaCl for arsenic) and ambient temperature (22−25 °C).

In order to study the effect of background electrolytes on arsenic removal efficiency of IMCS, three different salts (0.01 M NaCl, Na_2SO_4, and Na_3PO_4) were used. The experiments were done as described earlier but at pH 8 only. The effect of ionic strength on the adsorption of arsenic onto IMCS was tested at constant pH 8.0 and dosage (0.25 g) with the ionic strength ranging from 0.001 to 0.1 M NaCl. The adsorption kinetics studies of arsenic and phosphate onto the different adsorbents were carried out at the same conditions as previous stated but for a set amount of time, varying from 1 to 24 h.

A variation of dosage of each adsorbent ranging from 0.1 to 1.0 g was used to study the adsorption isotherms of arsenic or phosphate onto ICS, MCS, and IMCS with an initial pH 7 (at which most treatment is commonly performed). Adsorption results were fitted with Langmuir and Freundlich equations to determine best fit.

In order to compare adsorption efficiencies of ICS, IMCS, and MCS to the removal efficiency of phosphate by precipitation, two different salts of multivalent metal ions (precipitator) such as alum and $FeCl_3$ were used to form precipitates of sparingly soluble phosphate at different molar ratios of precipitator/phosphate. Chemical precipitation of phosphate by a metal precipitator was performed at constant pH (6 and 7, a typical treatment condition for drinking water) and ionic strength (0.01 M $NaNO_3$) with variation of molar ratio of precipitator/phosphate ranging from 0.5 to 4.0. In each experiment, the desired mass of precipitator was mixed with 500 mL of 2 mg/L phosphate. The solution pH was adjusted over the reaction time using 0.01 M HNO_3 and NaOH. The solution was mixed at 30 rpm for 24 h.

Analysis. To analyze arsenic concentrations, an anion-exchange resin column (Dowex 1 × 8 5−100) was used for the separation of As(III) and As(V). Fully protonated As(III) passed through the column while partly deprotonated As(V) was retained. The total dissolved arsenic concentration before the column separation and the As(III) concentration from the column effluent were measured via ICP-AES. The As(V) concentration was then calculated by mass balance. For phosphate, after 24 h, all samples were filtered, and then the residual phosphate concentration in the filtrate was measured with

a colorimeter (HACH DR/850). Analysis of variance (ANOVA) was used to test the significance of results, and $p < 0.05$ was considered to be statistically significant.

RESULTS AND DISCUSSION

Characterization of ICS, MCS, and IMCS. Figure 1 shows that the amounts of iron or manganese coated onto the sand

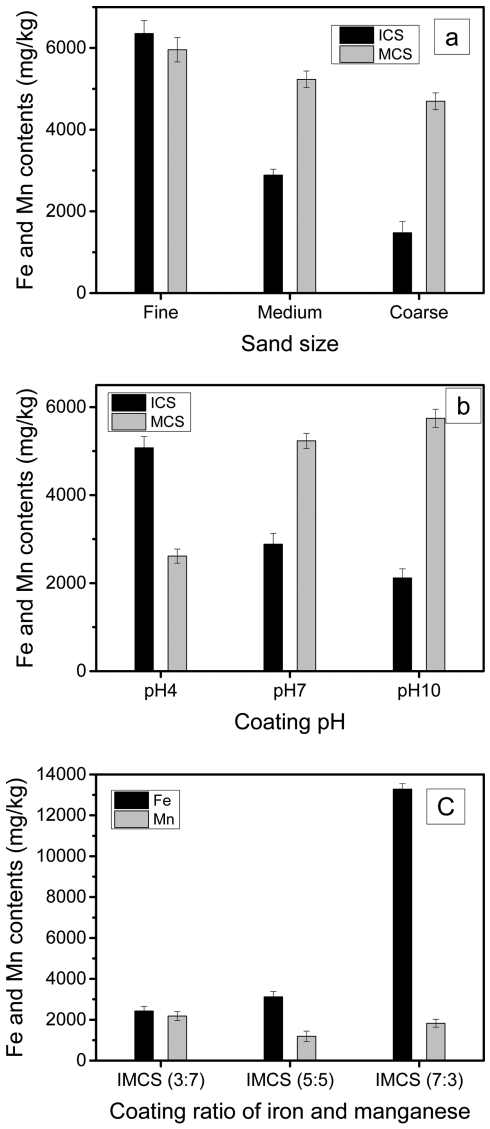

Figure 1. Iron and manganese contents in ICS and MCS prepared using different (a) sand size and (b) coating pH. (c) Iron:manganese ratio.

are dependent on preparation pH, sand size fraction, and iron to manganese ratio. The amounts of iron and manganese coated greatly increased as the sand size decreased for both ICS and MCS, especially for ICS (Figure 1a). ICS prepared with fine sand (100−125 μm) had four times greater amounts of iron coating than coarse sand (850−1000 μm). The amount of iron coated followed the same trend but was less sensitive to sand size. The amount of iron and manganese coated as a function of synthesis pH differed substantially for ICS and MCS (Figure 1b). The amount of iron coated on sand increased as solution pH decreased, while the amount of manganese coated decreased as solution pH decreased. This trend can be explained by the different solubility products of iron (Fe^{3+}) and manganese (Mn^{2+}) compounds depending on solution pH. Fe^{3+} can readily be precipitated below neutral pH,[23] while Mn^{2+} precipitates more at higher pH.[24] The optimized sand size (medium) and coating pH (4) was selected to synthesize IMCS, and then we used different ratios of iron and manganese to synthesize IMCS to compare the amounts of iron and manganese coated (Figure 1c). The estimated thickness of the coating varied from 123 nm to 1565 nm (Figure S1, Supporting Information).

SEM images of acid-washed sand in Figure 2a-1 show a relatively uniform and smooth surface. The ICS samples (Figure 2a) had much rougher surfaces than the raw sand. Relatively larger particles or agglomeration of particles were observed as coating pH increased in both ICS and MCS (Figure 2b). The same trend was observed for IMCS as the ratio of iron and manganese increased (Figure 2c).

Table 1 shows the specific surface area for raw sand, ICS, MCS, and IMCS prepared at different reaction parameters. The specific surface area of ICS samples increased as the solution pH decreased. On the contrary, the specific surface area of MCS samples increased as the solution pH increased. This trend correlated with trends of coating amounts of iron and manganese on sand at various solution pH.

Powders obtained from the same procedures for the preparation of ICS, MCS, and IMCS, but without the presence of sand, were used to analyze the mineral composition. Figure 3a, b, and c show X-ray diffraction spectra of iron and manganese oxides of ICS, MCS, and IMCS, respectively, using Cu Kα radiation (λ = 1.5406 Å) at kV = 40 and mA = 30, with a scan speed = 1.4 θ/min and scan range = 10−90 θ. The mineral type of ICS prepared at different solution pH was identified as a mixture of FeOOH and Fe_2O_3. The mineral type of MCS prepared at pH 4 and 7 was identified as MnO_2 and changed to ramsdellite (γ-MnO_2, a mixture of α-MnO_2 and β-MnO_2) at pH 10, as shown in Figure 3b. Figure 3c shows that the mineral type of IMCS prepared at different ratios of iron and manganese was a mixture of MnO_2 and FeOOH.

Table 2 shows pH_{pzc} values of ICS and MCS prepared at different coating pH with medium-sized sand as well as IMCS prepared at different ratios of iron and manganese. Similar to the XRD measurements, the powders obtained from the same procedures for the preparation of ICS, MCS, and IMCS, without the presence of sand, were used to measure pH_{pzc}. The pH_{pzc} values of ICS were above neutral pH and decreased as the coating pH increased, while pH_{pzc} values of MCS were below neutral pH and increased as the coating pH increased, although only slightly. pH_{pzc} values for different IMCS were below neutral pH. The variable pH_{pzc} values of ICS, MCS, and IMCS at different coating pH reflect the variation of deposited mineral type as observed in Figure 3.

Batch Adsorption of Phosphate. Figure 4a shows removal of phosphate by ICS, IMCS(7:3), and MCS at various solution pH. Adsorption of phosphate increased as the solution pH decreased, following a typical anionic adsorption behavior.[25] This trend is explained by the amphoteric properties of the surface (S−) functional groups (S−OH_2^+, S−OH, S−O^-) on the three adsorbents as well as the aqueous speciation of phosphate. The surfaces of ICS, IMCS, and MCS are positively charged below pH_{pzc}[25] (Table 2). From the simulation of the aqueous speciation of phosphate by MINEQL+ software, phosphate is mostly present as a neutral species (H_3PO_4, pK_{a1} = 2.1) at low pH (2.1 ± 0.5), while it is present as negative ions

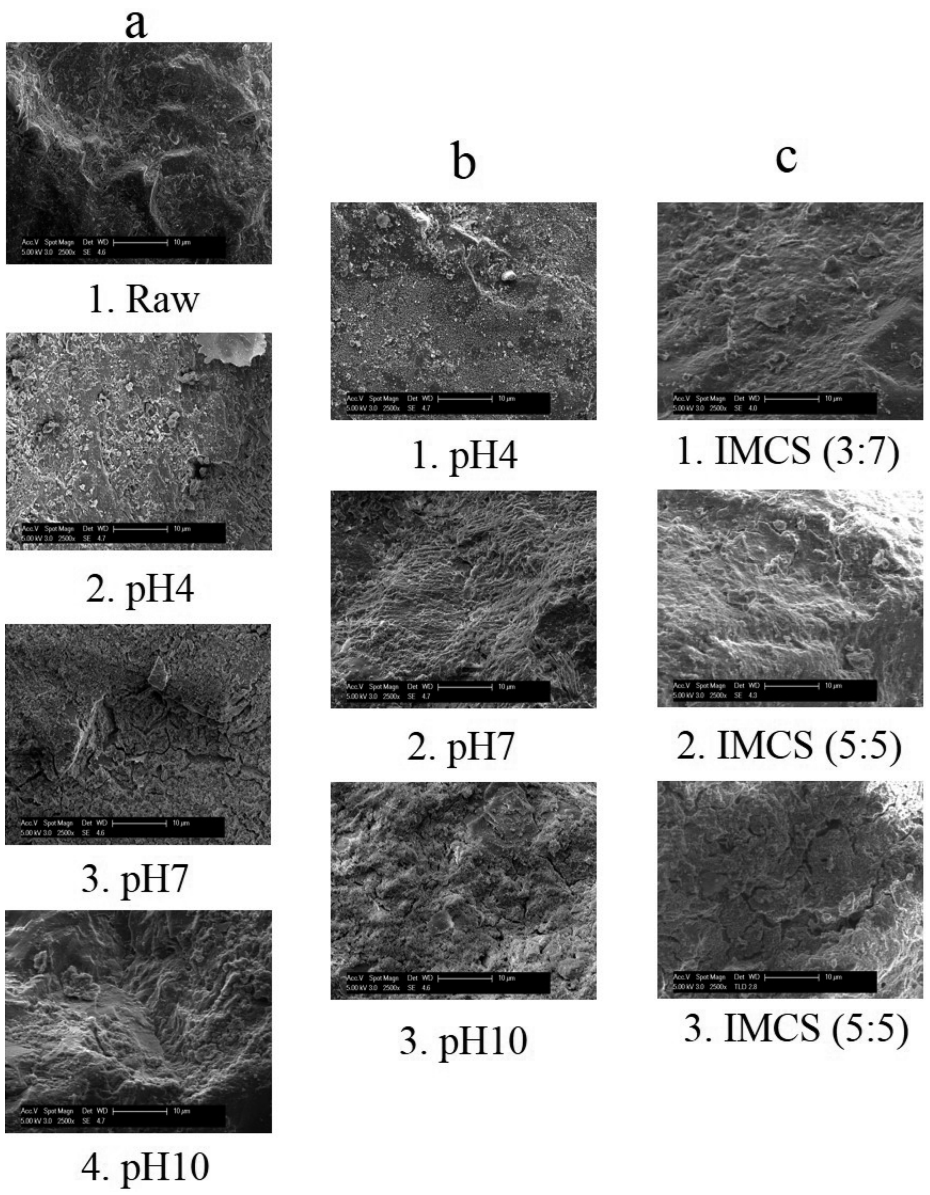

Figure 2. SEM images (2500×) of (a) ICS prepared at different coating pH, (b) MCS prepared at different coating pH, and (c) IMCS prepared at different ratios of iron and manganese. Magnification is 2500×, and scale bar is 10 μm.

Table 1. Specific Surface Area of Various Materials Using Medium Size Sand

	specific surface area (m^2/g)		
sample	pH 4	pH 7	pH 10
ICS	3.54	2.70	2.09
IMCS(7:3)	3.68	–	–
IMCS(5:5)	3.05	–	–
IMCS(3:7)	2.36	–	–
MCS	1.89	2.24	2.41
raw sand		2.13	

such as $H_2PO_4^-$ and HPO_4^{2-} (pK_{a2} = 7.2 and pK_{a3} = 12.3, respectively) between pH 3 and 10. Phosphate is essentially fully deprotonated (PO_4^{3-}) above pH 12.3. Thus, most phosphate was present as $H_2PO_4^-$ and HPO_4^{2-} in the pH range used in this study. Of all the adsorbents studied, ICS showed the greatest phosphate removal capacity below pH 5, with near complete phosphate removal. The adsorption capacity of MCS was five times less than that of ICS. Figure 4a clearly shows that iron (oxyhydr-)oxides have a greater adsorption capacity for phosphate than manganese oxide.

Figure 4b shows results for phosphate removal by addition of salts of multivalent metal ions (precipitator) to form precipitates of sparingly soluble phosphate at different molar ratios of precipitator/phosphate at neutral pH. Phosphate removal gradually increased with increasing molar ratios of precipitator/phosphate but decreased above a molar ratio of 3. Phosphate removal was distinctly increased in the presence of ferric chloride over the entire range of molar ratios. This is related to the different solubility constants between metal ions and phosphate species[26] as shown in Table 3. The precipitation chemistry of phosphate by iron or aluminum ions is quite complex due to the formation of various metal phosphate and metal hydroxyl complexes, as well as adsorption of phosphate onto the precipitates.[27] It was also reported that either metal phosphate precipitation alone occurs or both metal hydroxide and metal phosphate precipitation occurs depending on the

dx.doi.org/10.1021/sc400484s | ACS Sustainable Chem. Eng. 2014, 2, 1128−1138

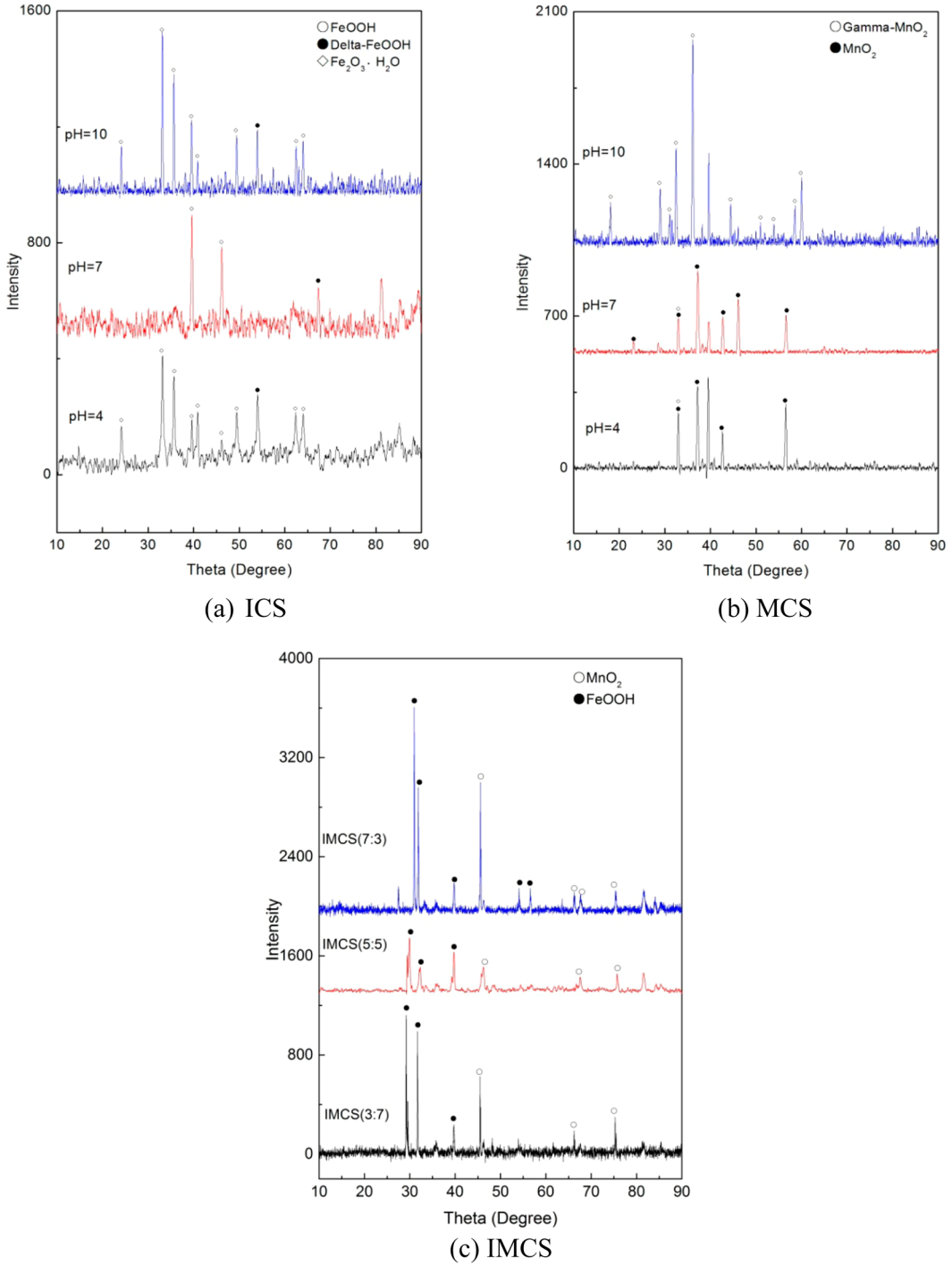

Figure 3. XRD patterns of (a) ICS and (b) MCS prepared at different coating pH, and (c) IMCS prepared at different ratios of iron and manganese.

Table 2. pH_{pzc} Values of ICS, MCS, and IMCS Prepared at Different pH with Medium Size Sand

	pH_{pzc}		
sample	pH 4	pH 7	pH 10
ICS	8.61 ± 0.08	7.67 ± 0.11	7.16 ± 0.07
IMCS(7:3)	4.62 ± 0.07	–	–
IMCS(5:5)	3.59 ± 0.23	–	–
IMCS(3:7)	5.81 ± 0.12	–	–
MCS	6.35 ± 0.16	6.67 ± 0.06	6.85 ± 0.10

dose ratio of precipitator/phosphate.[27] Phosphate removal in the presence of metal precipitators also depends on solution pH. At pH 7, the greatest phosphate removal was observed, with residual soluble phosphate of 1.79 mg/L for aluminum and 0.89 mg/L for Fe (III). Onthe basis of these results, ICS was identified as a favorable adsorbent with a greater removal capacity for phosphate than precipitation by alum or $FeCl_3$ below neutral pH. At higher pH, ICS is better than precipitation except high loading of $FeCl_3$, at a molar ratio of 3 or greater.

Removal of As(III) by ICS, MCS, and IMCS in a Batch Reactor. Figure 5a shows adsorption of arsenic onto ICS,

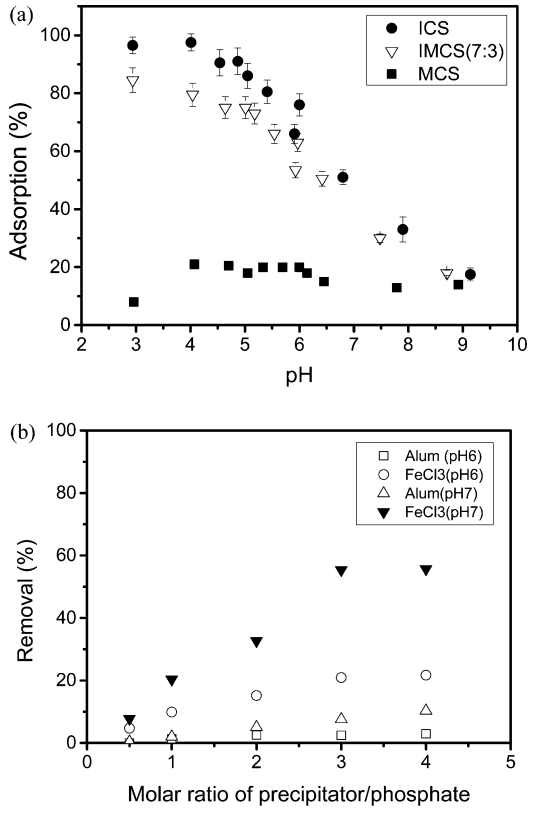

Figure 4. Removal of phosphate (a) by adsorption process using three different adsorbents and (b) by precipitation using two different precipitators (adsorbent dose = 5 g/L; ionic strength = 0.01 M $NaNO_3$).

Table 3. Solubility Constants for Forming Complexes and Solids from Metal Ions and Phosphate[26]

reaction	solubility constant
$Fe^{3+} + H_2PO_4^- = [FeH_2PO_4]^{2+}$	log K = 23.9
$Fe^{3+} + HPO_4^{2-} = [FeHPO_4]^+$	log K = 22.2
$Fe^{3+} + PO_4^{3-} = [FePO_4]$	log K = 26.4
$Al^{3+} + PO_4^{3-} = [AlPO_4]$	log K = 20.01

MCS, IMCS(7:3), IMCS(5:5), and IMCS(3:7), and Figure 5b shows As(III) oxidation to As(V) by these metal (hydr-)oxide coated sands at various solution pH. Metal (hydr-)oxide coated sands exhibit maximum As(III) removal near neutral pH because of the speciation of As(III) as well as the amphoteric properties of the surface of ICS. As(III) is mostly present as a neutral species (H_3AsO_3, pK_{a1} = 9.2) at low pH, while it is present as negative ions such as H_2AsO^{3-} at higher pH. The surface of metal (hydr-)oxide coated sand is positively charged below its pH_{pzc} and is negatively charged above pH_{pzc} (Table 2). Therefore, As(III) adsorption onto metal (hydr-)oxide coated sand is not electrostatically favorable at high pH due to similar charges or at very acidic conditions where As(III) and the surface of metal (hydr-)oxide coated sand have neutral charges. However, As(III) oxidation to As(V) in solution is also a function of pH (Figure 5b), resulting in increased removal of total arsenic because adsorption of As(V) is favorable.

The removal capacity follows the trend IMCS(7:3) > IMCS(5:5) > IMCS(3:7) > ICS > MCS. IMCS with both iron and manganese on the sand media exhibited better removal capacity of arsenic than ICS or MCS. This trend can

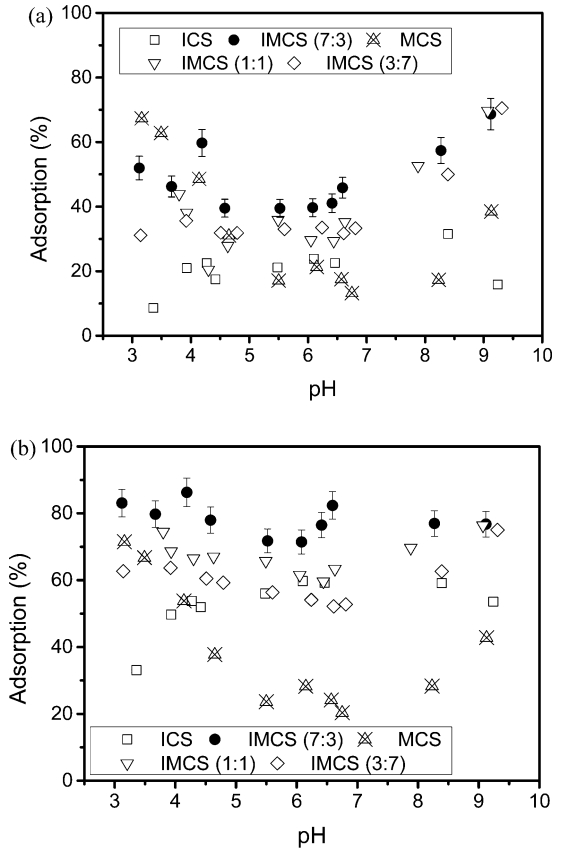

Figure 5. (a) Adsorption of arsenic onto ICS, IMCS(7:3), MCS, IMCS(5:5), and IMCS(3:7) and (b) oxidation in solution as a function of pH.

be explained by the favorable oxidation of As(III) to As(V) at higher coating of manganese oxide (Figure 1) and favorable adsorption of both remaining As(III) and generated As(V) onto the surface of IMCS. On the basis of the removal of total arsenic and the efficiency of oxidizing As(III) in solution, IMCS(7:3) is the best media to apply for the treatment of As(III).

Figure 6a shows the removal trends for As(III) onto IMCS(7:3) as well as the oxidized fraction of As(III) in solution as a function of ionic strength. Arsenic removal through phase transfer or oxidation was not significantly influenced by the significant variation of ionic strength. This trend may suggest that arsenic adsorption onto IMCS occurs mainly through inner-sphere complexes between arsenic and the surface functional group of IMCS.[28−30]

Figure 6b shows the removal efficiency of As(III) by IMCS(7:3) as well as the oxidation fraction of As(III) in solution with three different background electrolytes. As the formal charge increased, arsenic removal by IMCS(7:3) was greatly decreased especially in the presence of PO_4^{3-}. This trend could be explained by the increased competitive adsorption between arsenic and phosphate onto the limited surface sites on IMCS(7:3). In the presence of PO_4^{3-}, about a 50% reduction in arsenic removal was observed. Because PO_4^{3-} and AsO_4^{3-} have similar chemical structures, these two species might be in strong competition to occupy the finite number of adsorption sites on IMCS(7:3). A similar inhibition effect was reported for arsenic adsorption onto iron hydroxides.[31,32] A valid question is whether the oxidation from As(III) to As(V)

dx.doi.org/10.1021/sc400484s | ACS Sustainable Chem. Eng. 2014, 2, 1128−1138

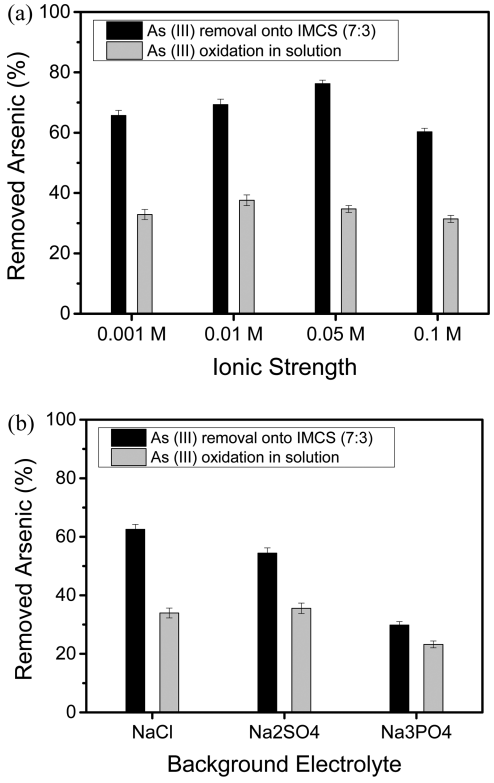

Figure 6. Removal of arsenic onto IMCS(7:3) at pH 6.5 (a) as a function of ionic strength and (b) in the presence of different background electrolytes.

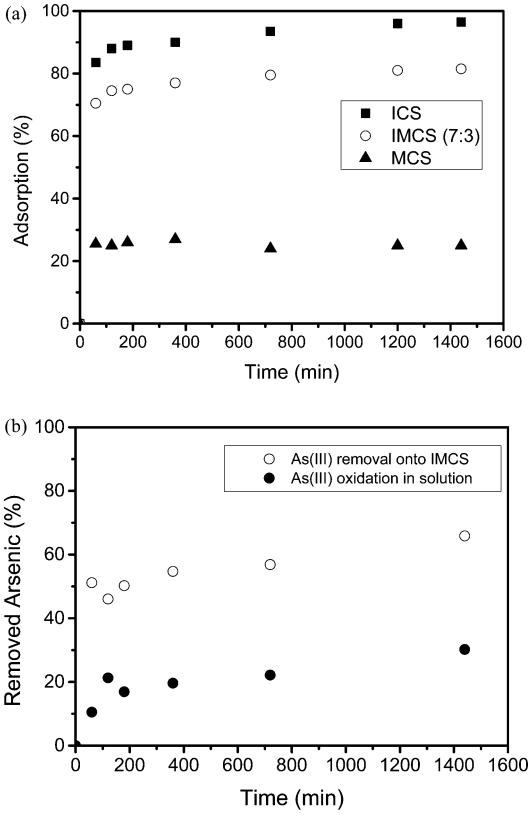

Figure 7. Adsorption of (a) phosphate onto ICS, IMCS(7:3), and MCS at pH 4.5 and (b) arsenic onto IMCS(7:3) at pH 6.5 as a function of time.

occurred in the oxic solution prior to the interaction with the adsorbent. A study of the kinetics of oxidation of As(III) to As(V) in the oxic solution, without adsorbents, showed that oxidation was only 2−7% in 24 h (Supporting Information). Thus, we believe that the As(III) in solution was adsorbed to the surface first and then oxidized to As(V). We also determined that IMCS(7:3) has a significant adsorption capacity for As(V) of 163 mg/kg, which is about half of the 326 mg/kg for As(III) (Figure S2, Supporting Information).

Removal Kinetics of Phosphate and Arsenic. Time-dependent phosphate removal results are shown in Figure 7a. The adsorption of phosphate onto three different adsorbents was rapid initially and then slowed as equilibrium was approached. The amounts of phosphate removed by ICS, IMCS(7:3), and MCS after 24 h were 386, 326, and 100 mg/kg, respectively. The kinetics results were used to study the rate-limiting step in the adsorption process.[33] The studied adsorption kinetic data of phosphate on the adsorbent was analyzed in terms of pseudo-first-order and pseudo-second-order sorption equations. A rate constant (k_1) for phosphate adsorption was determined from the following first-order rate expression[34]

$$\log(q_e - q_t) = \log(q_e) - \left(\frac{k_1}{2.303}\right)t \quad (1)$$

where q_e and q_t (both mg/kg) are the amount of phosphate adsorbed per unit mass of adsorbent at equilibrium and at specific reaction time t, respectively, and k_1 is the first-order rate constant (min^{-1}). The value of k_1 was calculated from the slope of the linear plot of $\log(q_e - q_t)$ versus time (data not shown). From this plot, the rate constants for phosphate adsorption onto ICS, IMCS(7:3), and MCS were determined as 1.84×10^{-3}, 2.30×10^{-3}, and 4.61×10^{-4} min^{-1}, respectively. However, the correlation coefficients of the linearity (r^2) were below 0.635 for the three adsorbents.

Because the first-order correlation coefficients were very low, second-order rate constants for phosphate adsorption were determined from the following rate expression[35]

$$\frac{1}{q_e - q_t} = \frac{1}{q_e} + k_2 t \quad (2)$$

which can be rearranged to

$$\frac{t}{q_t} = \frac{1}{k_2 q_e^{\,2}} + \frac{1}{q_e}t \quad (3)$$

where k_2 is the equilibrium rate constant of pseudo-second order sorption kinetics (kg/mg min). $k_2 q_e^{\,2}$ in the pseudo-second order equation can be expressed as the initial removal rate (h). Initial removal rate (h) and the pseudo-second order rate constant (k_2) were obtained from a linear correlation between t/q_t and t. The k_2 values for ICS, IMCS(7:3), and MCS were determined as 1.96×10^{-4}, 2.56×10^{-4}, and 6.91×10^{-4} kg/mg min, respectively. The correlation coefficients were above 0.995 for all three adsorbents. This indicates that the second-order rate constants increased as the fraction of manganese oxides on the sand surface increased. The values of h were calculated as 29.0 mg/kg min for ICS, 26.6 mg/kg min for IMCS(7:3), and 8.2 mg/kg min for MCS. As the linear corelation coefficients for the pseudo-second order rate expressions were much better than from the first-order rate expressions, it suggests that the removal of phosphate by these

three adsorbents follows pseudo-second order rate. The pseudo-second order rate constants, amount of phosphate adsorbed per unit mass of adsorbent at equilibrium, initial removal rate, and linear correlation coefficients are summarized in Table 4.

Table 4. Kinetic Parameters for Adsorption of Phosphate by ICS, IMCS(7:3), and MCS

adsorbent	k_2 (kg/mg min)	q_e (mg/kg)	h (mg/kg min)	r^2
ICS	1.96×10^{-4}	384.6	29.0	0.999
IMCS(7:3)	2.56×10^{-4}	322.6	26.6	0.999
MCS	6.91×10^{-4}	108.7	8.2	0.995

Figure 7b shows the removal trends for As(III) onto IMCS(7:3) as a function of time. Initial adsorption was fast and efficient compared to previous studies,[22,36,37] around 50% removal was obtained within 60 min, and stabilized at 66% removal after 24 h. The amount of As(III) removed by IMCS(7:3) was 151.5 mg/kg at pH 6.5. This value was smaller than the q_e value (322.6 mg/kg) for phosphate using IMCS(7:3) at pH 4.5 (Table 4). It may be explained by differences in affinity of these ions to the surfaces, as well as differences in pH change during adsorption runs. As(V), which may be generated from oxidation of As(III) by IMCS(7:3), may favorably adsorb onto IMCS(7:3) at the lower pH similar to our observation for phosphate (Figure 5). As the reaction time increases, the oxidized fraction of As(III) in solution not removed by IMCS(7:3) is slightly increased, likely due to the presence of manganese oxide on the surface of IMCS(7:3).[38]

Adsorption Isotherm of Phosphate and Arsenic. Adsorption isotherms of phosphate onto ICS, MCS, and IMCS(7:3) were obtained at pH 4.5 and 7 and at constant ionic strength (0.01 M $NaNO_3$) as shown in Figure 8a and b. MCS shows the least removal capacity for phosphate. Adsorption isotherm data with ICS and IMCS(7:3) were fitted using Langmuir and Freundlich adsorption isotherm models as shown in Figure 9. The Langmuir isotherm is expressed by eq 4[39]

$$q = \frac{abC_e}{1 + aC_e} \tag{4}$$

where C_e is the solute concentration (mg/L) at equilibrium, and q is the amount adsorbed (mg/kg). The Langmuir constant a represents the monolayer adsorption capacity (mg/kg), and b represents the strength and affinity of the adsorbent for the solute. The values of a and b calculated from the slope and intercept of the linear plot of C_e/q versus C_e are shown in Table 5. Results of adsorption experiments in this study showed that the maximum adsorption capacities of phosphate onto ICS and IMCS(7:3) were 693.08 and 593.42 mg/kg, respectively.

The Freundlich isotherm is expressed by eq 5[39]

$$\log q = \log K + \frac{1}{n}\log C_e \tag{5}$$

where q is the amount of adsorbed (mg/kg), C_e is the equilibrium solute concentration in solution (mg/L), and K and $1/n$ are the adsorption capacity and adsorption intensity, respectively. Langmuir and Freundlich isotherm constants for phosphate adsorption on two adsorbents are summarized in Tables 5 and 6, respectively.

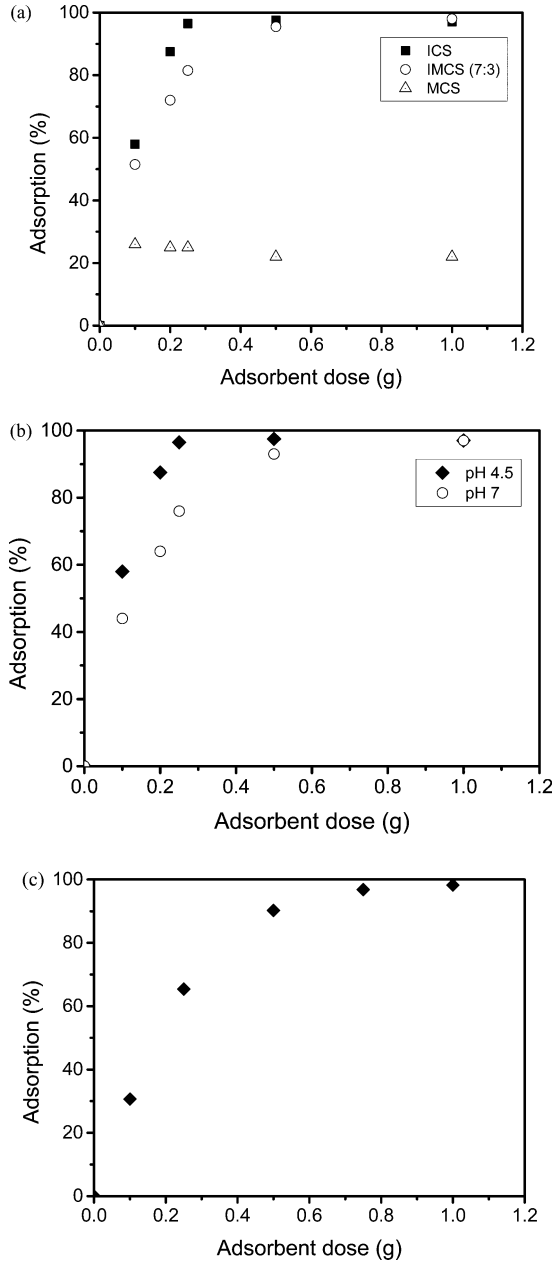

Figure 8. Adsorption of phosphate onto (a) ICS, IMCS(7:3), and MCS at pH 4.5, (b) ICS at pH 4.5 and pH 7, and (c) arsenic onto IMCS(7:3) at pH 7 as a function of adsorbent dose.

Adsorption isotherms of arsenic onto IMCS(7:3) were obtained at pH 7 and constant ionic strength (0.01 M NaCl) as shown in Figure 8c. Arsenic removal gradually increased with increasing adsorbent dose and reached a 90% removal rate above a dose of 0.5 g. The adsorption isotherm data was fitted using Langmuir and Freundlich adsorption isotherm models as shown in Figure 10. Langmuir and Freundlich isotherm constants for arsenic adsorption on two adsorbents are summarized in Tables 5 and 6, respectively.

While both Langmuir and Freundlich isotherms provided a good fit for the adsorption isotherm data, phosphate adsorption by IMCS(7:3) was best fit using the Langmuir adsorption isotherm model, and the Freundlich isotherm was a better fit for arsenic adsorption.

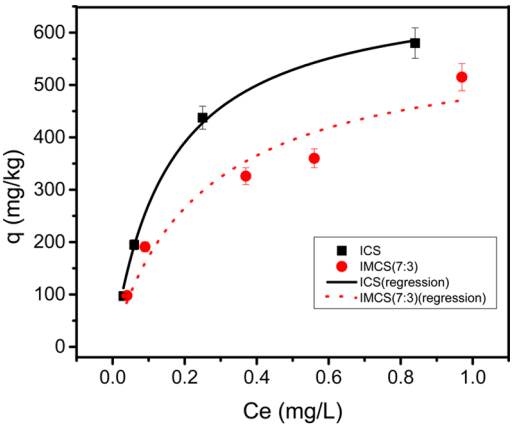

(a) Langmuir

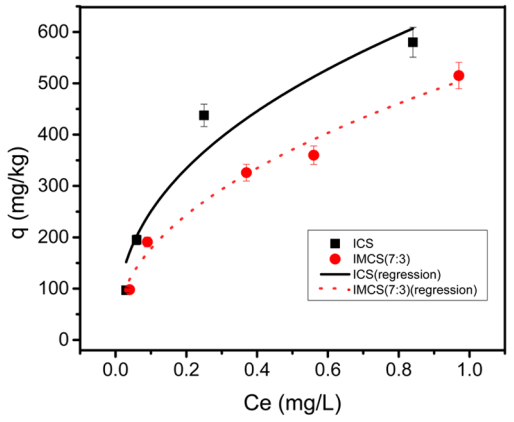

(b) Freundlich

Figure 9. (a) Langmuir and (b) Freundlich adsorption isotherms of phosphate on ICS and IMCS(7:3). Symbols represent experimental data, and lines represent model prediction.

Table 5. Langmuir Parameters and Correlation Constants for Phosphate and Arsenic Adsorption

	adsorbent	a (L/mg)	b (mg/kg)	r^2
phosphate	ICS	6.44	693.08	0.996
phosphate	IMCS(7:3)	3.98	590.42	0.915
arsenic	IMCS(7:3)	22.20	139.52	0.941

Table 6. Freundlich Parameters and Correlation Constants for Phosphate and Arsenic Adsorption

	adsorbent	$1/n$	K	r^2
phosphate	ICS	0.13	594.3	0.999
phosphate	IMCS(7:3)	0.50	513.1	0.962
arsenic	IMCS(7:3)	0.21	152.9	0.998

Environmental Significance. Inexpensive metal (hydro-)oxide adsorbents with a sand core were synthesized. Deposition of Fe onto sand was favored by finer sand fractions and lower synthesis pH. In contrast, a higher synthesis pH resulted in more deposition of Mn on sand. The BET surface area increased with metal oxide coating. The mineral type of ICS prepared at different solution pH was identified as a mixture of FeOOH and Fe_2O_3. The mineral type of MCS prepared at pH 4 and 7 was identified as MnO_2 and changed to ramsdellite (γ-MnO_2, a mixture of α-MnO_2 and β-MnO_2) at pH 10. To optimize the synthesis conditions for IMCS, pH 4 and medium-sized sand were selected to enhance the amount of iron and manganese coated as well as the adsorption capacity of As. The mineral type of IMCS was identified as a mixture of MnO_2 and FeOOH. By optimizing the coating step (i.e., lowering the coating temperature), a more sustainable low-cost metal (hydro-)oxide adsorbent synthesis method was developed.

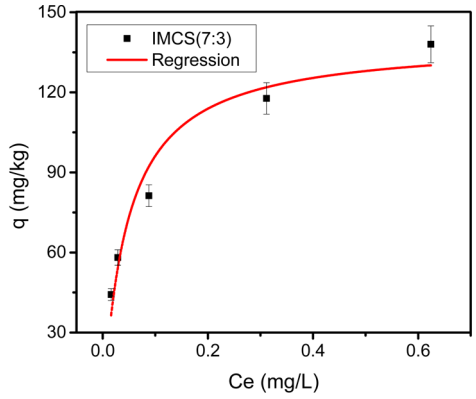

(a) Langmuir

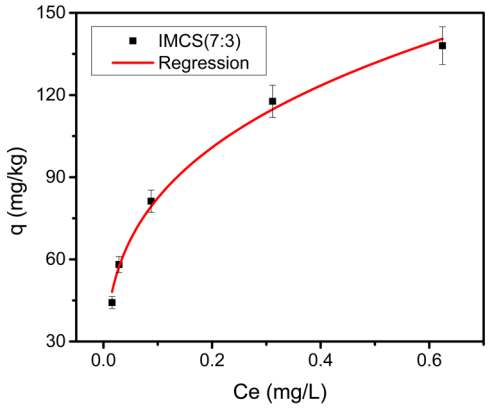

(b) Freundlich

Figure 10. (a) Langmuir and (b) Freundlich adsorption isotherms of arsenic on IMCS(7:3). Symbols represent experimental data, and lines represent model prediction.

ICS is a much better adsorbent of phosphate than MCS or IMCS for all ratios of iron and manganese in IMCS. ICS was also shown to have higher phosphate removal efficiency and capacity (up to 322 mg/kg at pH 7) than metal-based precipitators such as alum or Fe (III), even at precipitator/phosphate molar ratios greater than 3. The removal efficiency of phosphate increases significantly as pH decreases, with removal near 100% below pH 4. Removal of phosphate by ICS, MCS, and IMCS(7:3) followed the pseudo-second order model and the Langmuir adsorption isotherm. ICS can be used to meet the more stringent phosphate standards needed to reduce eutrophication of lakes and rivers around the world.

Compared to ICS and MCS, IMCS(7:3) is a more effective adsorbent for As(III), with fast initial removal within 60 min and 66% adsorption (132 mg/kg at pH 7) after 24 h. The adsorption and oxidation efficiency is significantly affected by pH, and the removal rate can achieve 90% removal at around pH 4. The removal efficiency of arsenic increases significantly as dose increases, with removal near 100% (up to 320 mg/kg) when 16 g/L IMCS(7:3) is used at pH 7. As(III) onto IMCS(7:3) was better represented by the Freundlich isotherm.

The background electrolytes are important factors in the As(III) oxidation and adsorption process.

■ ASSOCIATED CONTENT

Supporting Information

Experimental tables and graphs. This material is available free of charge via the Internet at http://pubs.acs.org.

■ AUTHOR INFORMATION

Corresponding Author

*Tel: +1 805 893 7548. Fax: +1 805 893 7612. E-mail: keller@bren.ucsb.edu.

Notes

The authors declare no competing financial interest.

■ ACKNOWLEDGMENTS

This work made use of the MRL Central Facilities supported by the MRSEC Program of the National Science Foundation under awards DMR 1121053 and DMR05-20415.

■ REFERENCES

(1) Ravenscroft, P.; Brammer, H.; Richards, K. *Arsenic Pollution: A Global Synthesis*; John Wiley & Sons: New York, 2011; Vol. *94*.

(2) Smedley, P. L.; Kinniburgh, D. G. A review of the source, behaviour and distribution of arsenic in natural waters. *Appl. Geochem.* **2002**, *17*, 517−568.

(3) Bhattacharya, P.; Welch, A. H.; Stollenwerk, K. G.; McLaughlin, M. J.; Bundschuh, J.; Panaullah, G. Arsenic in the environment: Biology and chemistry. *Sci. Total Environ.* **2007**, *379*, 109−120.

(4) Das, B.; Rahman, M. M.; Nayak, B.; Pal, A.; Chowdhury, U. K.; Mukherjee, S. C.; Saha, K. C.; Pati, S.; Quamruzzaman, Q.; Chakraborti, D. Groundwater arsenic contamination, its health effects and approach for mitigation in West Bengal, India and Bangladesh. *Water Qual., Exposure Health* **2009**, *1*, 5−21.

(5) Shrestha, R. R.; Shrestha, M. P.; Upadhyay, N. P.; Pradhan, R.; Khadka, R.; Maskey, A.; Maharjan, M.; Tuladhar, S.; Dahal, B. M.; Shrestha, K. Groundwater arsenic contamination, its health impact and mitigation program in Nepal. *J. Environ. Sci. Health, Part A: Toxic/Hazard. Subst. Environ. Eng.* **2003**, *38*, 185−200.

(6) *Guidelines for Drinking-Water Quality: First Addendum to Third ed., Vol. 1, Recommendations*; World Health Organization: Geneva, Switzerland, 2006.

(7) Mandal, B. K.; Suzuki, K. T. Arsenic round the world: A review. *Talanta* **2002**, *58*, 201−235.

(8) Mohan, D.; Pittman, C. U., Jr. Arsenic removal from water/wastewater using adsorbents—a critical review. *J. Hazard. Mater.* **2007**, *142*, 1−53.

(9) Sullivan, C.; Tyrer, M.; Cheeseman, C. R.; Graham, N. J. D. Disposal of water treatment wastes containing arsenic - A review. *Sci. Total Environ.* **2010**, *408*, 1770−1778.

(10) Meharg, A. A.; Hartley-Whitaker, J. Arsenic uptake and metabolism in arsenic resistant and nonresistant plant species. *New Phytol.* **2002**, *154*, 29−43.

(11) Hasegawa, H.; Sohrin, Y.; Seki, K.; Sato, M.; Norisuye, K.; Naito, K.; Matsui, M. Biosynthesis and release of methylarsenic compounds during the growth of freshwater algae. *Chemosphere* **2001**, *43*, 265−272.

(12) Gimenez, J.; Martinez, M.; de Pablo, J.; Rovira, M.; Duro, L. Arsenic sorption onto natural hematite, magnetite, and goethite. *J. Hazard. Mater.* **2007**, *141*, 575−580.

(13) Zhang, F. S.; Itoh, H. Iron oxide-loaded slag for arsenic removal from aqueous system. *Chemosphere* **2005**, *60*, 319−325.

(14) Chang, Y. Y.; Kim, K. S.; Jung, J. H.; Yang, J. K.; Lee, S. M. Application of iron-coated sand and manganese-coated sand on the treatment of both As(III) and As(V). *Water Sci. Technol.* **2007**, *55*, 69−75.

(15) Vohla, C.; Koiv, M.; Bavor, H. J.; Chazarenc, F.; Mander, U. Filter materials for phosphorus removal from wastewater in treatment wetlands−A review. *Ecol Eng.* **2011**, *37*, 70−89.

(16) Zhao, D. Y.; Sengupta, A. K. Ultimate removal of phosphate from wastewater using a new class of polymeric ion exchangers. *Water Res.* **1998**, *32*, 1613−1625.

(17) Arias, M.; Da Silva-Carballal, J.; Garcia-Rio, L.; Mejuto, J.; Nunez, A. Retention of phosphorus by iron and aluminum-oxides-coated quartz particles. *J. Colloid Interface Sci.* **2006**, *295*, 65−70.

(18) Genz, A.; Kornmuller, A.; Jekel, M. Advanced phosphorus removal from membrane filtrates by adsorption on activated aluminium oxide and granulated ferric hydroxide. *Water Res.* **2004**, *38*, 3523−3530.

(19) Han, Y. U.; Lee, C. G.; Choi, N. C. Phosphate removal from aqueous solution by aluminum (Hydr) oxide-coated sand. *Environ. Eng. Res.* **2009**, *14*, 164−169.

(20) Kabayama, M.; Sakiyama, T.; Kawasaki, N.; Nakamura, T.; Araki, M.; Tanada, S. Characteristics of phosphate aluminum oxide hydroxide for ion adsorption-desorption onto preventing eutrophication. *J. Chem. Eng. Jpn.* **2003**, *36*, 499−505.

(21) *Review of the EPA's Economic Analysis of Final Water Quality Standards for Lakes and Flowing Waters in Florida*; The National Academies Press: Washington, DC, 2012.

(22) Chang, Y. Y.; Lim, J. W.; Yang, J. K. Removal of As(V) and Cr(VI) in aqueous solution by sand media simultaneously coated with Fe and Mn oxides. *J. Ind. Eng. Chem.* **2012**, *18*, 188−192.

(23) Musić, S.; Orehovec, Z.; Popović, S.; Czakó-Nagy, I. Structural properties of precipitates formed by hydrolysis of Fe^{3+} ions in $Fe_2(SO_4)$ 3 solutions. *J. Mater. Sci.* **1994**, *29*, 1991−1998.

(24) McBride, M. Electron spin resonance investigation of Mn^{2+} complexation in natural and synthetic organics. *Soil Sci. Soc. Am. J.* **1982**, *46*, 1137−1143.

(25) Antelo, J.; Avena, M.; Fiol, S.; Lopez, R.; Arce, F. Effects of pH and ionic strength on the adsorption of phosphate and arsenate at the goethite-water interface. *J. Colloid Interface Sci.* **2005**, *285*, 476−486.

(26) Stumm, W.; Morgan, J. *Aquatic Chemistry: Chemical Equilibra and Rates in Natural Waters*; John Wiley & Sons: Hoboken, NJ, 1996.

(27) Li, C. J.; Ma, J.; Shen, J. M.; Wang, P. Removal of phosphate from secondary effluent with Fe^{2+} enhanced by H_2O_2 at nature pH/neutral pH. *J. Hazard. Mater.* **2009**, *166*, 891−896.

(28) Goldberg, S.; Johnston, C. T. Mechanisms of arsenic adsorption on amorphous oxides evaluated using macroscopic measurements, vibrational spectroscopy, and surface complexation modeling. *J. Colloid Interface Sci.* **2001**, *234*, 204−216.

(29) Waychunas, G. A.; Rea, B. A.; Fuller, C. C.; Davis, J. A. Surface chemistry of ferrihydrite 0.1. EXAFS studies of the geometry of coprecipitated and adsorbed arsenate. *Geochim. Cosmochim. Acta* **1993**, *57*, 2251−2269.

(30) Fendorf, S.; Eick, M. J.; Grossl, P.; Sparks, D. L. Arsenate and chromate retention mechanisms on goethite 0.1. Surface structure. *Environ. Sci. Technol.* **1997**, *31*, 315−320.

(31) Violante, A.; Pigna, M. Competitive sorption of arsenate and phosphate on different clay minerals and soils. *Soil Sci. Soc. Am. J.* **2002**, *66*, 1788−1796.

(32) Yang, J. K.; Song, K. H.; Kim, B. K.; Hong, S. C.; Cho, D. E.; Chang, Y. Y. Arsenic removal by iron and manganese coated sand. *Water Sci. Technol.* **2007**, *56*, 161−169.

(33) Khaodhiar, S.; Azizian, M. F.; Osathaphan, K.; Nelson, P. O. Copper, chromium, and arsenic adsorption and equilibrium modeling in an iron-oxide-coated sand, background electrolyte system. *Water, Air, Soil Pollut.* **2000**, *119*, 105−120.

(34) Lagergren, S. Y. *Zur Theorie der sogenannten Adsorption gelöster Stoffe*; 1898.

(35) Coleman, N. T.; Mcclung, A. C.; Moore, D. P. Formation Constants for Cu(Ii)-Peat Complexes. *Science* **1956**, *123*, 330−331.

(36) Chang, Y. Y.; Song, K. H.; Yang, J. K. Removal of As(III) in a column reactor packed with iron-coated sand and manganese-coated sand. *J. Hazard. Mater.* **2008**, *150*, 565−572.

(37) Chang, Y. Y.; Lee, S. M.; Yang, J. K. Removal of As(III) and As(V) by natural and synthetic metal oxides. *Colloid Surf., A* **2009**, *346*, 202−207.
(38) Oscarson, D.; Huang, P.; Liaw, W. Role of manganese in the oxidation of arsenite by freshwater lake sediments. *Clays Clay Miner.* **1981**, *29*, 219−225.
(39) Morel, F. M. M.; Hering, J. G. *Principles and Applications of Aquatic Chemistry*; John Wiley & Sons: New York1993.